

# EXTENDED CONSTITUTIVE RULES FOR VARIOUS VISCOELASTIC MATERIALS USING FRACTIONAL DERIVATIVES

Y. Ooki<sup>1)</sup> and K. Kasai<sup>2)</sup>

1) *Research Associate, Structural Engineering Research Center, Tokyo Institute of Technology, Japan*

2) *Professor, Structural Engineering Research Center, Tokyo Institute of Technology, Japan*  
*ooki@serc.titech.ac.jp, kasai@serc.titech.ac.jp*

**Abstract:** This paper discusses the constitutive rule including the fractional time-derivatives of the strain and stress. We have modeled four kinds of constitutive rules of viscoelastic materials based on this, and introduce the typical material of acrylic and styrene material here. Although viscoelastic material has temperature and frequency sensitivity, accurate modeling is possible by using temperature-frequency equivalency principle. Furthermore, efficient modeling is conducted to reproduce the behavior under large strain without spoiling accuracy. The behavior of the material under sinusoidal or random excitation was examined by comparing the experiment and analysis results. The proposed model showed high accuracy.

## 1. INTRODUCTION

Dynamic characteristics of viscoelastic (VE) material used for dampers are linear under small strain loading but vary according to the ambient temperature and frequency. In addition, the material shows nonlinear behavior when it is subjected to large strain loading. Since the loading strain in VE material varies in time especially under seismic loading, accurate analytical models for time-history analysis are required for the design of viscoelastically-damped buildings.

The linear VE model based on the fractional time-derivatives of the stress and strain (fractional derivative model) is proposed (Kasai et al, 2001) and this model shows high accuracy compared with the traditional integer derivative models. Based on the temperature-frequency equivalency principle (Ferry, 1980) of VE material, “equivalent frequency” is proposed to consider the complex interactions between the temperature and frequency sensitivities efficiently. On the other hand, various nonlinear models have been proposed (Soda et al, 2002). Usually in those models, the temperature, frequency, and strain sensitivities are considered separately, and it has been difficult to model the accurate constitutive rule which reproduce those three sensitivities in wide range.

In this paper, linear and nonlinear models including the fractional time-derivatives of the stress and strain are discussed. Further more, the use of temperature-frequency equivalency principle has lead to excellent model accuracy. The accuracy is examined compared with the various loading test results and time-history analyses under various excitations. We have modeled four kinds of constitutive rules of VE materials, and will discuss the typical two types, acrylic and styrene material.

## 2. LINEAR CONSTITUTIVE RULES FOR SMALL STRAIN

### 2.1 Temperature-Frequency Equivalency Principle

Consider a given damper deformation  $u(t)$  and force  $F(t)$ , corresponding shear strain  $\gamma(t)$  and stress  $\tau(t)$  are

$$\gamma(t) = u(t)/d, \quad \tau(t) = F(t)/A_s \quad (1a, b)$$

where  $d$  and  $A_s$  are VE material thickness and shear area, respectively. Fig. 1 shows typical linear steady-state response of a VE material subjected to sinusoidal shear deformation. VE material is often characterized by the storage modulus  $G'$  and the loss factor  $\eta$ .

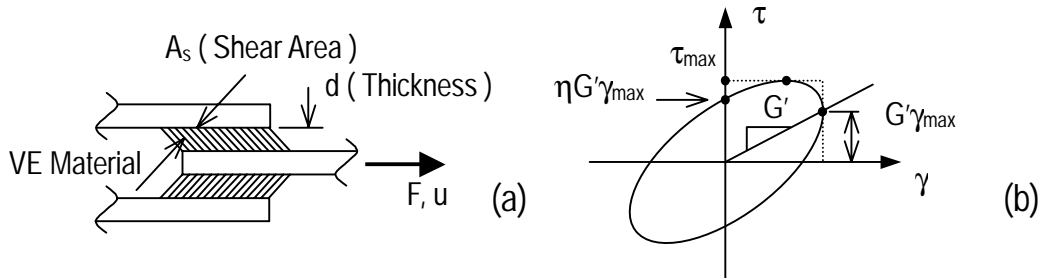


Figure 1 (a) Shear Deformation and (b) Stress-Strain Curve of VE Material

Fig. 2 shows the  $G'$  and  $\eta$  at 10 % strain. Material properties vary according to the temperature and frequency.  $G'$  and  $\eta$  are large at low temperature or high frequency, and small at high temperature or low frequency. The test results at 0, 10, 20, 30, 40 °C are shown and all data can be overlapped into a curve at 20 °C by moving parallel to the horizontal axis. This characteristic is known as “temperature-frequency equivalency principle” and observed in the materials which we have ever treated.

$$G'(\omega, \theta) = G'(\lambda\omega, \theta_{ref}), \quad \eta(\omega, \theta) = \eta(\lambda\omega, \theta_{ref}) \quad (2a, b)$$

where  $\lambda$  is shifting factor and  $\lambda\omega/(2\pi)$  ( $=f_{eq}$ ) is defined as “equivalent frequency”. The amount of movements in Fig. 2 is equivalent to  $\log\lambda$ . By using the temperature-frequency equivalency, we have only to take into account the sensitivities for the equivalent frequency.

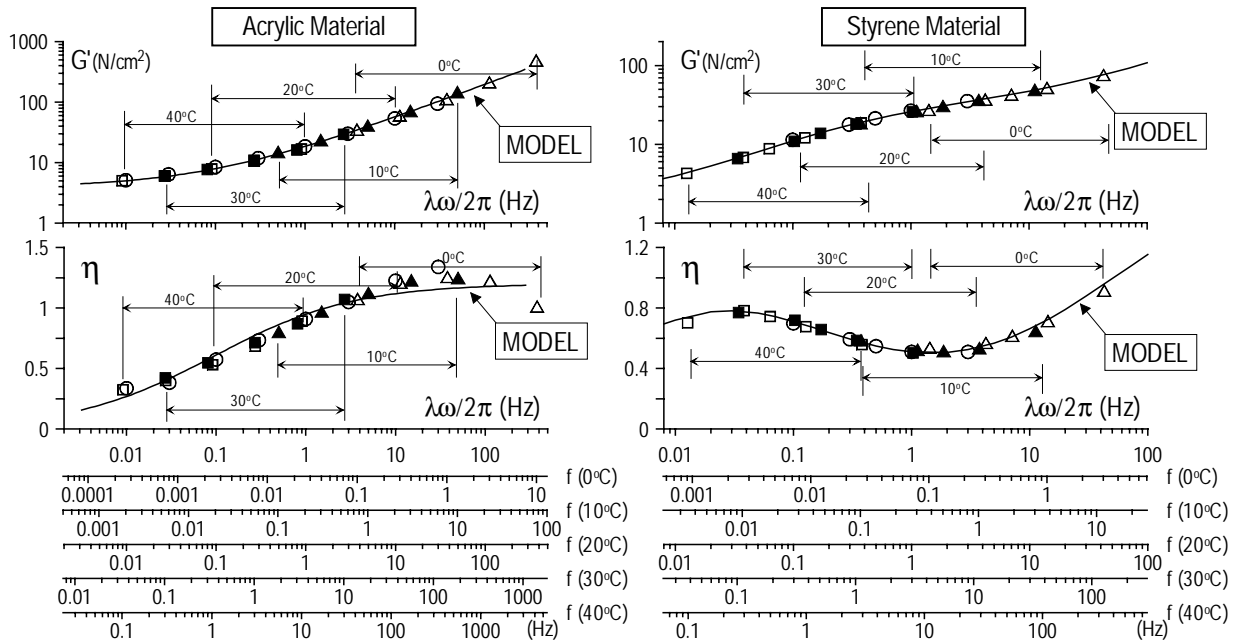


Figure 2 Experimental Results and Model at 20 °C, and Relationships between Temperature, Frequency, and Equivalent Frequency ( $\gamma_{max} = 10\%$ )

## 2.2 Linear Constitutive Rules Using Fractional Derivatives

The advantage of the fractional derivative rule as opposed to the more conventional integer derivative rule is the ability to model the VE material accurately over a large range of frequency with a small number of constants. The following is generalized model using fractional derivatives.

$$\tau(t) + \sum_n a_n D^{\alpha_n} \tau(t) = G [ \gamma(t) + \sum_n b_n D^{\beta_n} \gamma(t) ] \quad (3)$$

where  $a_n$  and  $b_n$  are constants,  $G$  is elastic parameter, and  $\alpha_n$  and  $\beta_n$  is the order of fractional derivative of stress and strain.  $D^\alpha$  ( $= d^\alpha/dt^\alpha$ ) is the fractional derivative operator. To satisfy the temperature-frequency equivalency shown in Eq. (2),

$$a_n = a_{n,ref} \lambda^{\alpha_n}, \quad b_n = b_{n,ref} \lambda^{\beta_n}, \quad \lambda = \exp [ -p_1(\theta - \theta_{ref}) / (p_2 + \theta - \theta_{ref}) ] \quad (4a, b)$$

where  $a_{n,ref}$  and  $b_{n,ref}$  are constants at reference temperature  $\theta_{ref}$  (20 °C). Eq. (5) and (6) are applied to acrylic and styrene material under small strain, and model for the acrylic material has four parameters;  $a_{ref} = 5.60 \times 10^{-5}$ ,  $b_{ref} = 2.10$ ,  $G_{ref} = 3.92 \times 10^{-2}$  (N/mm<sup>2</sup>), and  $\alpha = 0.56$  (Kasai et al. 2001). On the other hand, model for the styrene material has seven parameters;  $a_{ref} = 0.84$ ,  $b_{1,ref} = 0.94$ ,  $b_{2,ref} = 15.1$ ,  $G = 1.63 \times 10^{-2}$  (N/mm<sup>2</sup>),  $\alpha = 0.57$ ,  $\beta_1 = 1.24$ , and  $\beta_2 = 0.63$  (Kasai et al. 2003). Solid lines in Fig. (2) show the frequency sensitivities of the materials by the proposed models, and match well with experimental results.

$$\text{Acrylic Material:} \quad \tau(t) + aD^\alpha \tau(t) = G [ \gamma(t) + bD^\alpha \gamma(t) ] \quad (5)$$

$$\text{Styrene Material:} \quad \tau(t) + aD^\alpha \tau(t) = G [ \gamma(t) + b_1 D^{\beta_1} \gamma(t) + b_2 D^{\beta_2} \gamma(t) ] \quad (6)$$

### 3. EXTENDED CONSTITUTIVE RULES USING FRACTIONAL DERIVATIVES

#### 3.1 Temperature-Frequency Equivalency Principle under Large Strain

Fig. 3 shows hysteresis loops under different strain with same equivalent frequency (See Section 2.1). Nonlinearities such as softening and hardening are observed and the shape of hysteresis loops

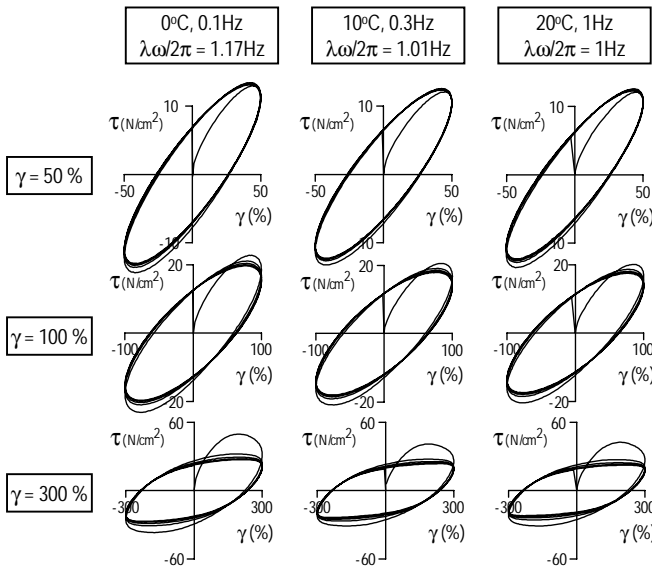


Figure 3 Temperature-Frequency Equivalency under Large Strain

look very similar. This indicates that the temperature-frequency equivalency is also applicable to nonlinear VE material modeling. Utilizing this finding, we have to only take into account the strain and equivalent frequency sensitivities (Fig. 4).

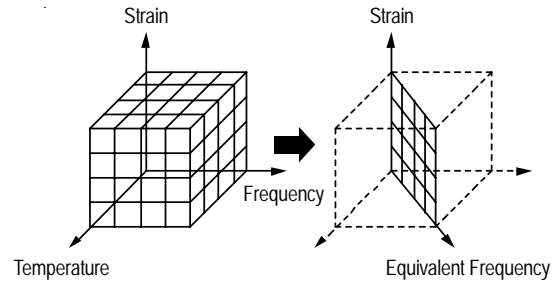


Figure 4 Reduction of Parameter Using Temperature-Frequency Equivalency

#### 3.2 Source of Nonlinearity

Four kinds of nonlinearity of VE material have been found from the experiment and are discussed in this paper. Fig. 5 shows the comparison of time-history responses and hysteresis loops between small and large strain tests, and strain is normalized by maximum value. In small strain test, temperature-rise is negligibly small and VE material behaves linearly. Characteristics of these nonlinearities are as follows;

**a) Softening by temperature-rise:**

Temperature-rise of VE material is significant under low ambient temperature. The  $G'$  and  $\eta$  gradually decreases with number of cycles.

**b) Softening by large strain:**

Reduction of  $G'$  is significant under large strain and  $\eta$  rises relatively in this case. This occurs without the temperature-rise and characterized difference softening mentioned above.

**c) Hardening by high strain-rate:** At the beginning of loading, the strain suddenly increases in very large rate, and abrupt increase in shear stress is observed. Especially, this occurs under high equivalent frequency with large strain.

**d) Hardening by large strain:** Hysteresis shows pinching if the shear strain advances further, This behavior is remarkable in the materials which have strong strain sensitivities.

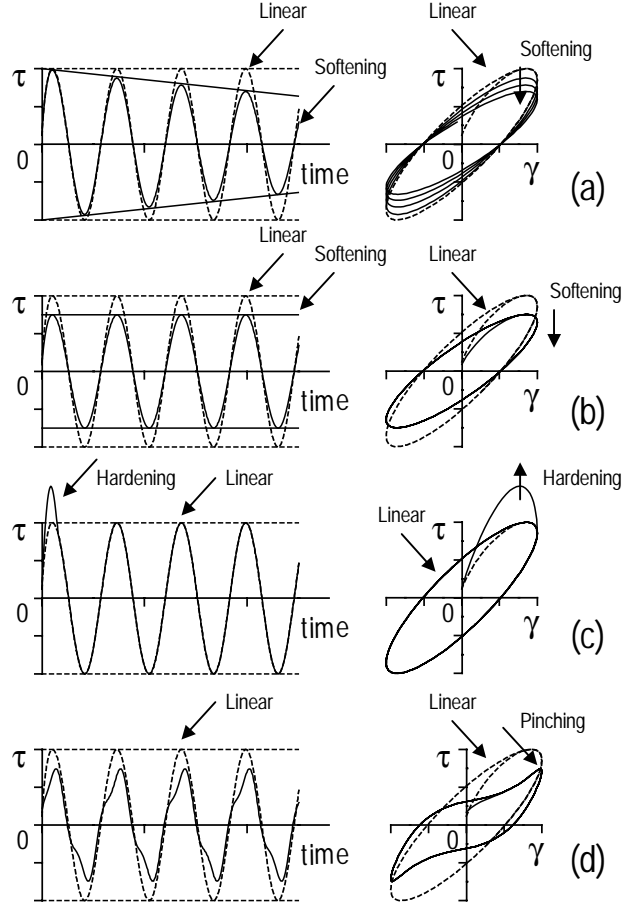


Figure 5 Nonlinearity of VE Material: (a) Softening by Temperature, (b) Softening by Large Strain, (c) Hardening by High Strain-Rate, and (d) Hardening by Large Strain (Pinching)

**3.3 Additional Components for Nonlinear Model**

**Acrylic Material:** The temperature  $\theta(t)$  in the VE material is evaluated using the shear stress, strain, density  $\rho$ , and specific heat,  $s$ , of the material as (Kasai et al, 1993)

$$\theta = \theta_0 + \int \tau d\gamma / (s\rho) \tag{7}$$

where  $\theta_0(t)$  is initial temperature. In Eq. (7), it is assumed that the heat generated in the VE material is all contained in VE material and heat loss due to heat conduction is ignored. This assumption is applied since the external loading time is short and the thermal conductivity of the material is small. Temperature-rise is calculated by using Eq. (7), shifting factor  $\lambda$  is changed by Eq. (4c), and  $a$  and  $b$  are updated by Eq. (4a) and (4b). Thus softening by temperature-rise is reproduced in numerical analysis.

In contrast with the softening phenomenon examined above, even when the temperature-rise is very small, the softening is seen at large strain with high temperature or low frequency, i.e., low equivalent frequency  $f_{eq} = \lambda\omega / (2\pi)$ . This is a softening caused by large strain shown in Fig. 5 previously. In the softening by the temperature-rise previously mentioned,  $\eta$  decreases with decreasing of  $G'$ . By increasing  $b$  and decreasing  $G$ , vice versa, in Eq. (5), the behavior can be reproduced, and this modeling is applied at  $\theta \geq 25$  °C and  $\gamma_{max} \geq 100$  % because softening by temperature-rise dominates in low temperature. The  $b$  and  $G$  vary almost linearly with respect to maximum strain at  $\gamma_{max} \geq 100$  % and modeled as follows;

$$b = b_{ref} \lambda^\alpha \lambda_1, \quad G = G_{ref} \lambda_2 \tag{8a, b}$$

$$\lambda_1 = 1 + C_1(\gamma_{max} - 1), \quad \lambda_2 = 1 + C_2(\gamma_{max} - 1) \tag{9a, b}$$

where  $C_1 = 0.124$  and  $C_2 = -0.182$ .

From temperature-frequency equivalency principle, strain-rate  $\dot{\gamma}$  at  $\theta$  is equivalent to  $\lambda\dot{\gamma}$  at  $\theta_{ref}$ . Accordingly,  $\lambda\dot{\gamma}$  is defined as “equivalent strain-rate”, and its maximum is  $\lambda\dot{\gamma}_{max}$ . Under sinusoidal loading,  $\lambda\dot{\gamma}_{max}$  occurs at the beginning of loading, and the hardening is effectively modeled by utilizing the data at the 1st half cycle. Nonlinear spring element is adopted parallel to the fractional derivative model to reproduce this phenomenon. Required spring stiffness  $G_s$  is written as

$$\tau_s = G_s \cdot \gamma \quad (10a)$$

$$G_s = C_3 \beta \min[\lambda\dot{\gamma}_{max}, 100], \quad \beta = \exp[C_4(\gamma_0 - 0.5)] \leq 1 \quad (10b)$$

where  $C_3 = 0.278$  (N·sec/cm<sup>2</sup>) and  $C_4 = -0.549$ .  $\gamma_0$  is absolute value of the strain when the sign of strain-rate changes.  $G_s$  is set to 0 after the unloading and not used until  $\lambda\dot{\gamma}_{max}$  is updated again.

The stress of the VE element  $\tau_v$  is obtained by substituting Eq. (8) for Eq. (5), and total stress  $\tau_{tot}$  considering the nonlinearity of the material is shown as follows.

$$\tau_{tot} = \tau_v + \tau_s \quad (11)$$

**Styrene Material:** Softening by the large strain of styrene material is reproduced by applying the parameter which is dependent on maximum strain  $\gamma_{max}$  to Eq. (6) same as the case of acrylic material.

$$a = a_{ref} \lambda_2^\alpha, \quad b_1 = b_{1,ref} \lambda_3^{\beta_1}, \quad b_2 = b_{2,ref} \lambda_4^{\beta_2}, \quad G = G_{ref} \lambda_1 \quad (12a, b, c, d)$$

$$\lambda_i = A_i \exp[B_i \gamma_{max}] \quad , \quad i = 1 \sim 4 \quad (13)$$

where  $A_i$  ( $i = 1 \sim 4$ ) = 1.11, 1.06, 1.081, and 1.03,  $B_i$  ( $i = 1 \sim 4$ ) = -0.58, -0.56, -0.78, and -0.30.  $\lambda_i$  decreases further by repeating cyclic loading with large strain. (Kasai et al, 2004)

Under large strain with low equivalent frequency, the material becomes stiff and pinching is observed in the hysteresis. To reproduce this, a spring is added parallel to the VE element and its stiffness depends on the strain. Stress with this spring is set to  $\tau_s$ .

$$\tau_s = G_s \cdot \gamma \quad (14a)$$

$$G_s = m_1 \gamma^3 + m_2 \gamma^2 + m_3 \gamma \quad (14b)$$

where  $m_i$  ( $i = 1 \sim 3$ ) = -0.23, 1.16, and -0.44.

Setting up the parameters as shown in Eq. (8), acrylic material can reproduce change of the loss factor under large strain, but in this material, which has strong strain sensitivities, a nonlinear dashpot is required to reproduce the behavior under large strain. Stress with this element is set to  $\tau_d$ .

$$\tau_d = C_1 \cdot C_2 [\lambda\dot{\gamma}]^\zeta \quad (15a)$$

$$C_1 = n_1 \gamma_0^3 + n_2 \gamma_0^2 + n_3 \gamma_0 \quad (15b)$$

$$C_2 = \min(C_t, \dot{\gamma} / \dot{\gamma}_{pk}) \quad , \quad C_t = |\sin \pi(\gamma - \gamma_0) / (2\gamma_0)|^\zeta \quad (15c, d)$$

where  $n_i$  ( $i = 1 \sim 3$ ) = -0.37, 1.55, and 0.89,  $C_1$  = function of  $\gamma_0$  ( $-3.0 < \gamma_0 < 3.0$ ) used in Eq. (10b).  $C_2$  = coefficient which starts from 0 and ends by 0 in a half cycle, and can take 1 as maximum.  $\dot{\gamma}_{pk}$  is strain-rate in a half cycle and set to 0 when the sign of strain-rate changes.  $C_t$  and  $\dot{\gamma}_{pk}$  are updated until it reaches maximum in a half cycle.  $\zeta = 0.26$ .

Eq. (7) is also applied for reproducing the softening by temperature-rise. The stress of the VE element  $\tau_v$  is obtained by substituting Eq. (12) for Eq. (6), and total stress  $\tau_{tot}$  considering the nonlinearity of the material is shown as follows;

$$\tau_{tot} = \tau_v + \tau_s + \tau_d \quad (16)$$

#### 4. COMPARISON BETWEEN ANALYSIS AND EXPERIMENT

Fig. 6 and 7 show the sinusoidal responses of two materials. The softening by temperature-rise is remarkable at low temperature or high frequency. Softening by large strain as well as hardening by high strain-rate is also reproduced in high accuracy by proposed model. The test at 0 °C is not conducted as for Acrylic material because of the limit of the performance of the testing machine. In Table 1, the accuracy of these two models is examined. Storage modulus and loss factor are compared between experiment and analysis. Not only the average of the ratio of the experiment and analysis is almost equal to 1, but also standard deviation is very small.

Fig. 8 and 9 show the case of random loading considering the events of JMA Kobe, El Centro and Taft earthquake. The ambient temperature 20 °C is considered and the maximum strains are set to 300 %. The deformation history is obtained from analyses of 3, 12, and 24 story buildings having fundamental vibrations of 0.35, 1.41, and 2.84 seconds. Note that the material stiffness and number of cyclic excursions differ significantly with respect to building's vibration periods. The analytical prediction matches extremely well with the experimental results.

#### 5. CONCLUSIONS

- 1) The temperature-frequency equivalency principle, the typical characteristic of VE material, is applicable not only under small strain range but also large strain range. It is possible to express the sensitivity of temperature and frequency as that of equivalent frequency.
- 2) The nonlinear behavior of the VE material characterized by softening by temperature-rise of material, softening by large strain, and hardening by high strain-rate. And pinching is observed if the material has strong strain sensitivity. The tendency of nonlinearity is effectively expressed by the equivalent frequency, which combines the effects of both temperature and frequency.
- 3) High accuracy of proposed analysis model was proved by performing comparison with the experiment over wide range temperature, frequency, and peak shear strain. This model also showed high accuracy for the random waves.

#### References:

- Kasai, K., Teramoto, M., Okuma, K., and Tokoro, K., "Constitutive Rule for Viscoelastic Materials Considering Temperature and Frequency Sensitivity", *Journal of Structural and Construction Engineering*, AIJ, No. 543, May, 2001, pp. 77-86 ( in Japanese )
- Ferry, J.D., *Viscoelastic Properties of Polymers*, John Wiley & Sons Inc., Third Ed., New York, 1980
- Soda, S., Kakimoto, K., and Sekiya, E., "Mechanical Models for Softening and Hardening Type Nonlinear Viscoelastic Dampers", *Journal of Structural and Construction Engineering*, AIJ, No. 551, 2002, pp. 45-52 ( in Japanese )
- Kasai, K., Munshi, J. A., Lai, M-L, and Maison, B.F., "Viscoelastic Damper Hysteresis Model: Theory, Experiment, and Application", ATC-17-1 Seminar, Applied Technology Council, Vol. 2, 1993, pp.521-532
- Kasai, K., Ooki, Y., Amemiya, K., and Kimura, K., "A Constitutive Rule for Viscoelastic Materials Combining Iso-Butyrene and Styrene Polymers", *Journal of Structural and Construction Engineering*, AIJ, No. 569, July, 2003, pp. 47-54 ( in Japanese )
- Kasai, K., Ooki, Y., and Amemiya, K., "Principles of Manual for Design and Construction of Passively-Controlled Buildings Part-11 Time-History Analysis Model for Viscoelastic Dampers Combining Iso-Butylene and Styrene Polymers, *Proceedings of 13th World Conference on Earthquake Engineering*, Vancouver, BC Canada, Aug. 1-6, 2004

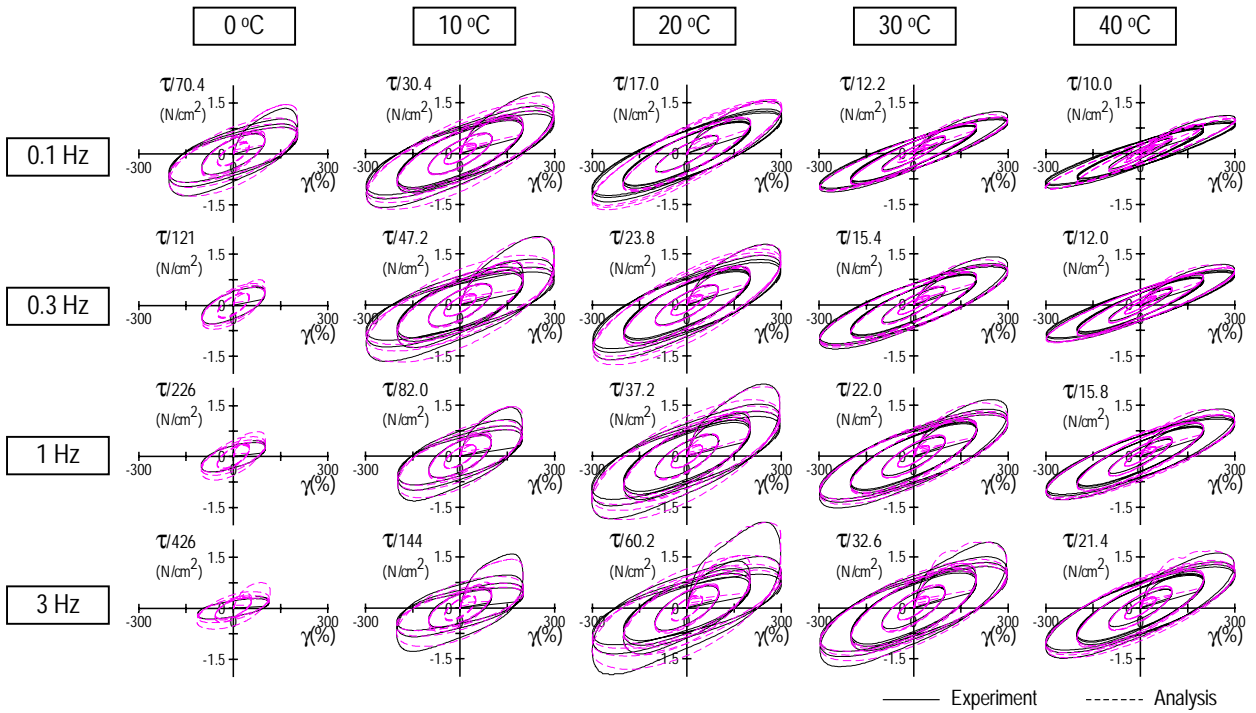


Figure 6 Sinusoidal Responses of Acrylic Viscoelastic Material ( $\gamma_{max} = 50, 100, 200, 300\%$ )

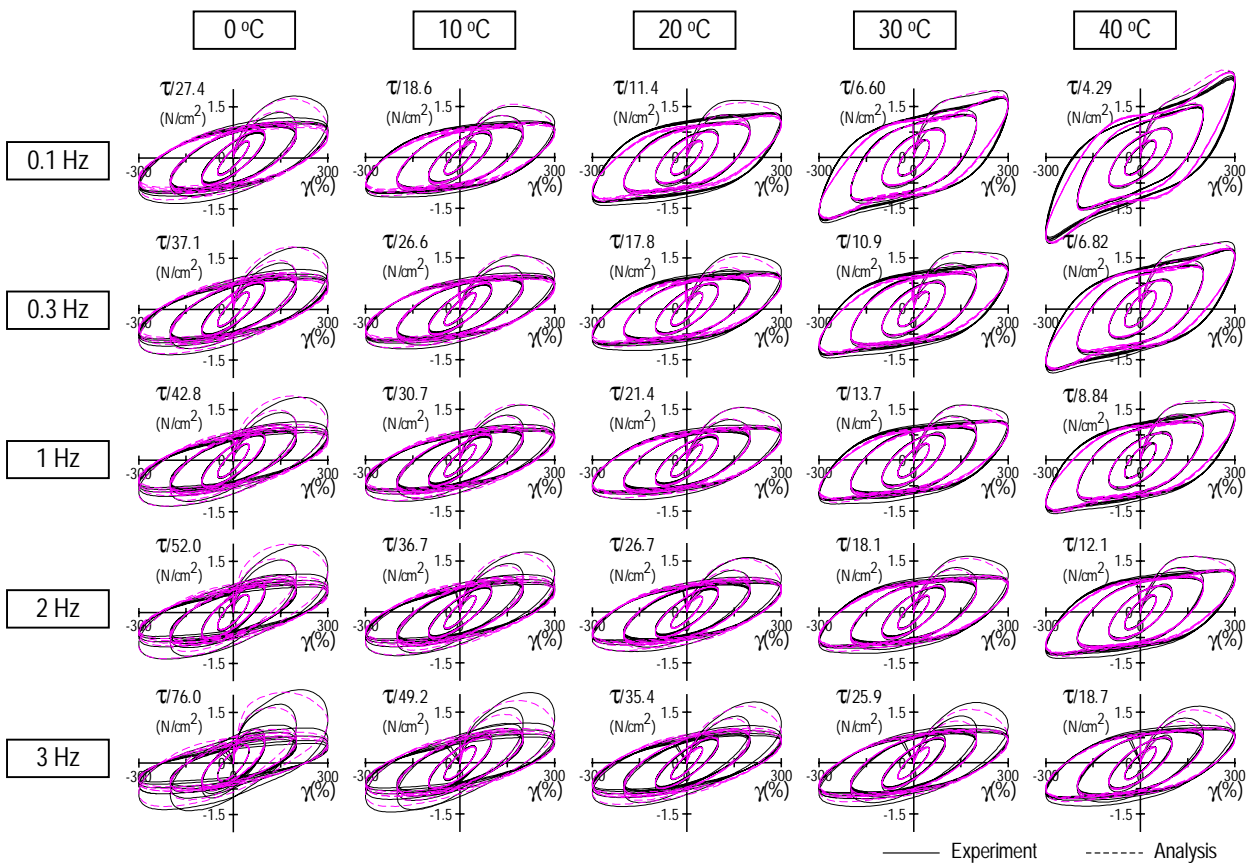


Figure 7 Sinusoidal Responses of Styrene Viscoelastic Material ( $\gamma_{max} = 50, 100, 200, 300\%$ )

Table 1 Accuracy Verification of Sinusoidal Responses: (a) Acrylic Material, (b) Styrene Material

Analysis/Test	$\gamma = 10\%$		$\gamma = 50\%$		$\gamma = 100\%$		$\gamma = 200\%$		$\gamma = 300\%$	
	$G'$	$\eta$	$G'$	$\eta$	$G'$	$\eta$	$G'$	$\eta$	$G'$	$\eta$
Average	1.02	1.02	1.02	0.98	1.04	0.99	0.99	1.05	0.96	1.08
Standard Dev.	0.050	0.090	0.033	0.077	0.054	0.074	0.098	0.108	0.087	0.125

(a)

Analysis/Test	$\gamma = 10\%$		$\gamma = 50\%$		$\gamma = 100\%$		$\gamma = 200\%$		$\gamma = 300\%$	
	$G'$	$\eta$	$G'$	$\eta$	$G'$	$\eta$	$G'$	$\eta$	$G'$	$\eta$
Average	0.99	1.00	0.99	1.00	1.03	0.97	1.05	0.97	0.96	1.02
Standard Dev.	0.019	0.028	0.020	0.037	0.044	0.038	0.060	0.029	0.034	0.047

(b)

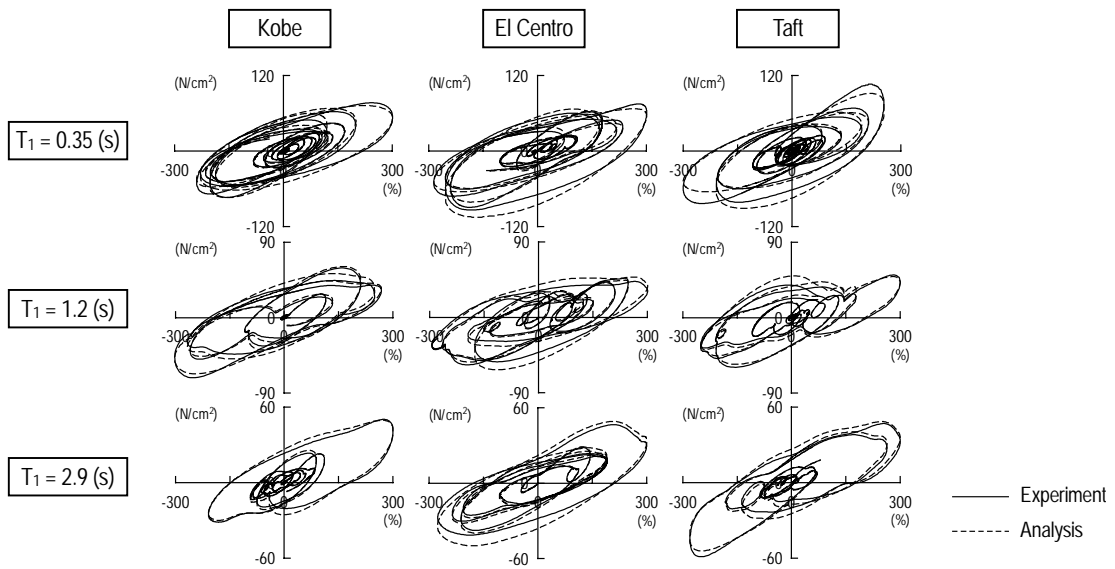


Figure 8 Responses of Acrylic Viscoelastic Material (Deformation history is obtained from analyses of 3, 12, and 24 story buildings having fundamental period of 0.35, 1.2, and 2.9 seconds)

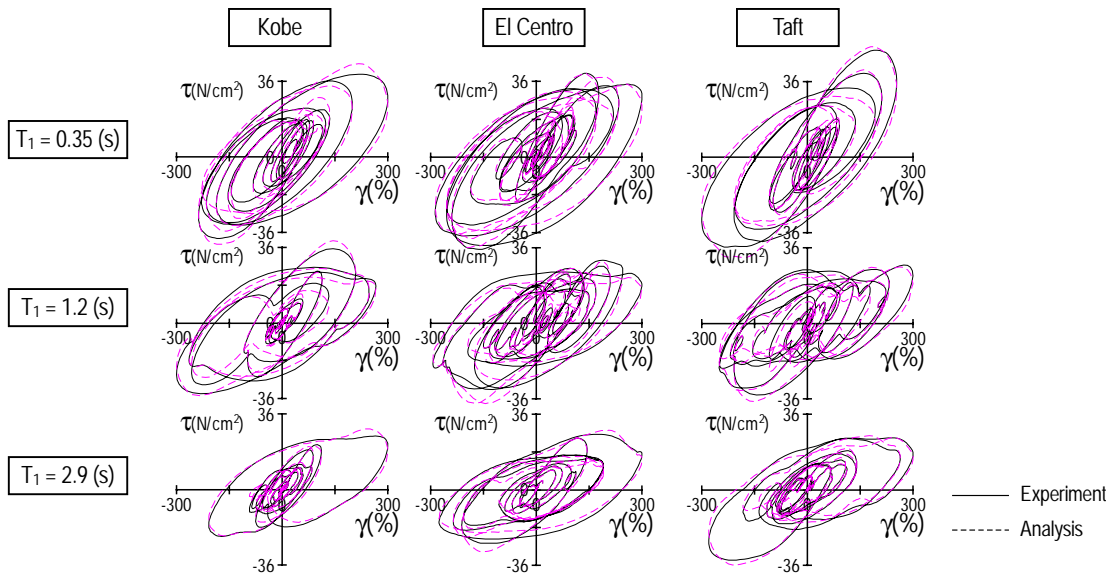


Figure 9 Responses of Styrene Viscoelastic Material (Deformation history is obtained from analyses of 3, 12, and 24 story buildings having fundamental period of 0.35, 1.2, and 2.9 seconds)